

# Qualifying optical inter-satellite links for atmospheric occultations

N. Perlot<sup>1</sup>, V. Sofieva<sup>2</sup>

<sup>1</sup>*DLR (German Aerospace Center), nicolas.perlot@dlr.de*

<sup>2</sup>*FMI (Finnish Meteorological Institute)*

## Abstract:

The Earth and its atmosphere obstruct optical links between near-Earth satellites, and determine the beginning and the termination of the links. Whereas optical inter-satellite communications are perturbed by the atmosphere, optical limb sounding has appeared to provide valuable information on the structure of the atmosphere. In this paper, we review the altitude-dependent atmospheric effects on the optical beam: attenuation, vertical defocusing, wavefront distortions and scintillation. Looking for synergies between atmospheric measurements and satellite communications, we discuss the possibility of adapting a laser communication terminal so that it can accurately measure atmospheric occultation effects.

## 1. Introduction

Optical links between near-Earth satellites are generally repeatedly obstructed by the Earth and its atmosphere. The atmospheric occultation can be as short as 20 seconds, or much longer depending on the satellite orbits. There are several motivations for characterizing the impact of the atmosphere on satellite optical links.

The air medium attenuates the optical signal and makes it randomly fluctuate. Communication terminals should be prepared for such effects and should not, for example, misinterpret an unexpected signal level (too low or too high). There is always a limit on the beam altitude under which communication is not possible. So, it is also of interest to maximize the communication time by setting the proper start and end of the transmission.

Optical occultation can also serve atmospheric research. Star light having propagated through the Earth atmosphere has already been observed from satellites and analyzed. Important deductions on atmospheric structure have then been made [1-4]. The main advantages of measuring the atmosphere through stellar occultation are [5]:

- self-calibration (propagations through air and vacuum can be compared)
- good vertical resolution
- good global coverage provided by the multitude of suitable star targets.
- wide altitude range of measurements (for absorption measurements, the altitude range from the upper troposphere up to thermosphere is covered; scintillation measurements can provide information about small-scale processes at altitudes 25-60 km, where other measurements with such vertical resolution are very scarce).

Active occultations (with lasers) might have some advantages over passive occultations (with stars). With an artificial source more power can be concentrated on

particular wavelengths. However, it has an additional implementation cost.

In this paper, we will first review the main properties of optical occultations (Sections 2 – 4), and then discuss the possibility of adapting a communication terminal to occultations (Section 5).

## 2. Link geometry

Fig. 1 shows the main geometrical parameters of the link.  $H_p$  is the altitude of the link perigee which is the point on the link path with shortest distance to the Earth. Along the path, we have  $L_1$  (resp.,  $L_2$ ) the distance from the transmitter (resp., receiver) to the perigee.  $L$  is the link distance ( $L = L_1 + L_2$ ). Let  $R_e = 6370$  km be the Earth radius. With  $H_p \ll R_e$ ,  $L$  can be assumed independent of  $H_p$ .

Mean air density decreases almost exponentially with altitude (the atmospheric scale height is  $\sim 7$ km). Therefore, the region of main interaction between light and atmosphere is located around the perigee of the optical ray. The horizontal length  $L_{eff}$  of this region is a few hundreds of kilometers [1]. To simplify analyses, the effect of extended atmosphere is replaced by that of a virtual phase screen located at the perigee and modelled as a thin screen. The thin phase screen approximation is valid if  $L_{eff} / 2 \ll L_1$  and  $L_{eff} / 2 \ll L_2$ .

## 3. Overview of atmospheric effects

Atmospheric effects on the optical beam are extinction, refraction, vertical defocusing and random wavefront distortions caused by random refractive-index variations.

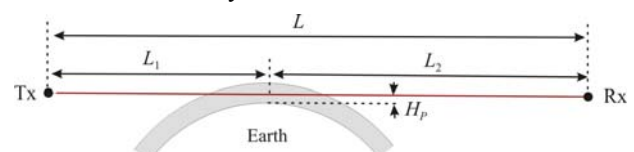
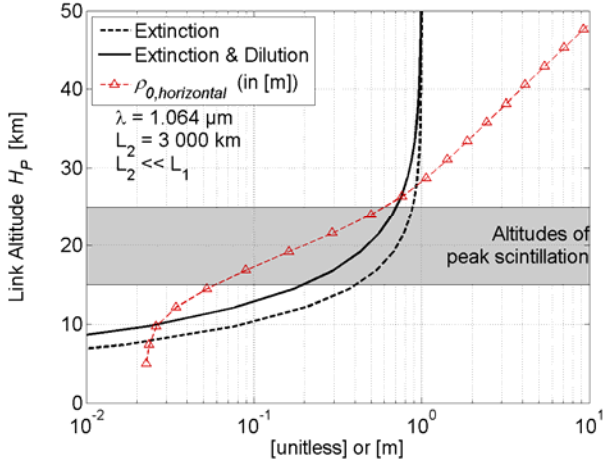


Fig. 1 Link geometry and parameters.



**Fig. 2 Estimation of some atmospheric effects as a function of link altitude and for the wavelength 1.064  $\mu\text{m}$ . The horizontal coherence width  $\rho_{0,\text{horizontal}}$  is based on Kolmogorov turbulence.**

Scintillation results from wavefront distortions and strengthens with subsequent propagation. Atmospheric effects tend to strengthen with decreasing altitude.

### 3.1. Extinction

Extinction is the attenuation caused by absorption and scattering in the (cloud-free) atmosphere. Extinction does not depend on  $L_1$  or  $L_2$ , and generally (not for all wavelengths) decreases exponentially with altitude. The extinction was estimated at  $\lambda = 1.064 \mu\text{m}$  from a database at DLR [6] and is displayed in Fig. 2 (dashed line).

### 3.2. Vertical defocusing (dilution)

The vertical layering of the mean refractive index causes an altitude-dependent refraction of optical rays, which in turn causes a vertical defocusing of the beam. The corresponding loss at the Rx-satellite is given by the dilution factor  $\phi$  with  $0 < \phi < 1$ . Considering a spherical wave, we have [7]

$$\phi^{-1} = 1 - \frac{L_1 L_2}{L} \frac{d\omega}{dh} \quad (1)$$

where  $d\omega/dh$  is the derivative of the refraction angle with respect to altitude. The combined loss due to extinction and dilution is shown as a solid line in Fig. 2 for the case  $L_1 L_2 / L = 3000 \text{ km}$  and  $\lambda = 1.064 \text{ nm}$ .

### 3.3. Wavefront distortions

Distortions of the received wavefront can perturb the link because the Rx-satellite perceives a fluctuating angle of arrival. Differences between vertical and horizontal distortions are expected due to the presence of gravity waves and vertical defocusing. Vertical distortions are increased by anisotropic irregularities and decreased by vertical defocusing. In Fig. 2, the horizontal coherence width  $\rho_{0,\text{horizontal}}$  is displayed (line with triangle markers) for  $\lambda = 1.064 \text{ nm}$  and  $L_2 \ll L_1$ . The horizontal coherence width was estimated from isotropic Kolmogorov

turbulence according to  $\rho_{0,\text{horizontal}} = (1.46k^2\mu_0)^{-3/5}$

where  $k = 2\pi/\lambda$  and  $\mu_0$  is the path-integrated  $C_n^2$  [8]. The  $C_n^2$  height profile is the HV<sub>5/7</sub> model (described e.g. in [9]) with an enhancement in the stratosphere according to [2][10]. Spatial coherence increases with the wave expansion and thus depends on the satellite position (i.e., on  $L_1$  and  $L_2$ ). Considering a spherical-wave expansion, we have the proportionality relations:

$$\begin{cases} \rho_{0,\text{horizontal}} \propto L / L_1 \\ \rho_{0,\text{vertical}} \propto \phi^{-1} L / L_1. \end{cases} \quad (2)$$

### 3.4. Scintillation

The difficulty of characterizing scintillation resides in the coexisting isotropic and anisotropic irregularities and in the saturation effect of scintillation. Theory and measurements in the near-infrared window show that saturation leads to a maximum of scintillation variance at altitudes 15-25 km (saturation occurs usually below  $\sim 25$  km; some reduction of the saturated scintillation variance is expected below  $\sim 15$  km, in the region of very strong scintillations). A scintillation index up to a value of 4 has been measured [11]. The altitude region of peak scintillation is displayed in Fig. 2.

For scenarios where the beam enters the atmosphere with a small diameter (e.g.  $\sim 10 \text{ m}$ ), beam wander [8] may significantly contribute to scintillation.

### 4. Time properties

The temporal behaviour of fluctuations depends on the satellite orbits. Links involving a circular LEO satellite and a slow remote satellite (e.g., GEO) are characterized by the angle  $\alpha_{\text{orbit}}$  made by the LEO plane with respect to the direction towards the remote counter-satellite. Fig. 3 shows, for two different  $\alpha_{\text{orbit}}$  angles, the LEO orbit as seen from the counter-satellite. In Fig. 4, the link altitude  $H_P$  is plotted versus time for different orbital passes (i.e., for different  $\alpha_{\text{orbit}}$  values). One observes that a grazing occultation (i.e., with  $\alpha_{\text{orbit}} \sim 75^\circ$ ) is longer than a central occultation (i.e., with  $\alpha_{\text{orbit}} \sim 0^\circ$ ).

Furthermore, in a grazing occultation the beam traverses the atmosphere rather horizontally whereas in a central occultation the atmosphere is traversed rather vertically. Due to anisotropic irregularities and vertical defocusing, the temporal spectrum of central and grazing occultations have different shapes.

Assuming a "frozen" atmosphere, the correlation time  $\tau_c$  of a fluctuating quantity (phase or intensity) depends on the quantity's correlation width  $\rho_c$  and the speed  $V$  of the optical ray through the atmosphere [8]. If the beam can be modelled as a plane wave and vertical defocusing is neglected, we can write  $\tau_c = \rho_c / V$ . E.g. with  $\rho_c = 1 \text{ m}$  and  $V = 2 \text{ km/s}$ , we have  $\tau_c = 500 \mu\text{s}$ . With decreasing altitude,  $\rho_c$  is expected to decrease and so is  $\tau_c$ . In order to fully capture the fluctuations of the optical wave, measuring devices with high frequency bandwidth are required.

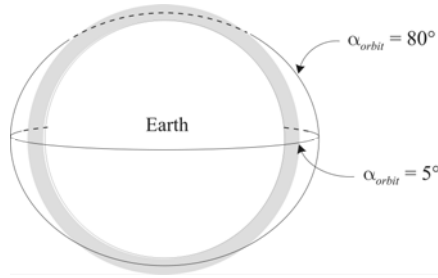


**Fig. 3 Geometry of an occultation link with a LEO satellite and a remote counter-satellite. The LEO orbit makes an angle  $\alpha_{orbit}$  with respect to the direction towards the counter-satellite. The LEO orbit is traced as seen from the counter-satellite for two different  $\alpha_{orbit}$  angles.**

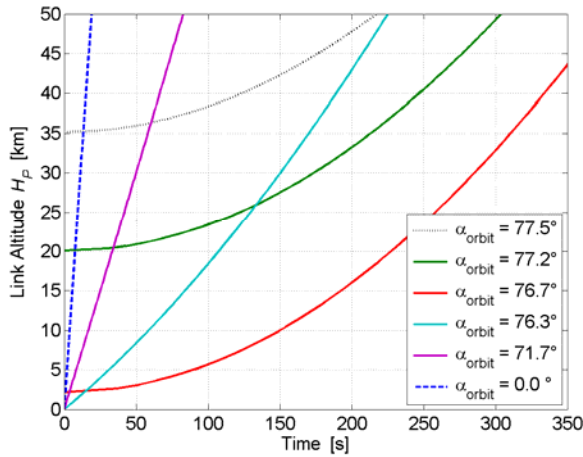


**Fig. 4 Link altitude  $H_p$  versus time for different orbital passes characterized by the angle  $\alpha_{orbit}$ . A link between a LEO satellite and a slow remote counter-satellite is assumed.**

## 5. Hybrid system for measurements and communications

For a standard laser communication terminal several modes (or phases) are possible during occultation: "Off", "Spatial acquisition", or "Communication". The terminal behaviour may be modified so that, in any of the above modes, atmospheric measurement is possible. The degree of synergy between the activities of atmospheric measurements and communications depends on the amount of common elements.

### 5.1. Satellite orbits

To couple both activities, the orbits of the lasercom satellites should fulfil the geographical requirements of atmospheric research (e.g., in terms of global coverage [12]). For example, experiments involving a GEO satellite are restricted to the exploration of the sky above a circular strip on the Earth surface. The strip mostly corresponds to a longitudinal band (except near the poles) surrounding the Earth and has a width that is given by the atmospheric sounding length  $L_{eff}$ . One can estimate the area of the strip surface as  $2\pi R_e L_{eff}$  and the percentage of Earth coverage as  $L_{eff} / 2R_e \approx 5\%$ . This Earth coverage may be reduced depending on the number of counter-satellites and on their orbits.

Another atmospheric-research requirement on orbits may be the restriction to central occultations or to grazing occultations.

### 5.2. Optical beam

Elements that should reasonably be in common are the telescopes and the pointing assemblies. The choice of using a common beam, hence a common wavelength, depends on the atmospheric property to be studied. Among atmospheric properties, two different types can be studied:

- 1) Atmospheric constituents (such as greenhouse gases:  $\text{CO}_2$ ,  $\text{CH}_4$ ,  $\text{N}_2\text{O}$ , ...)
- 2) Refractive-index variations corresponding to air density or temperature variations

If the presence of particular gases is to be detected, a communication wavelength is unlikely to be suitable (note that the wavelength of any beacon beam used for the establishment of a communication link is here included in the term "communication wavelength"). Gases are identifiable through their absorption spectra and so the measurement wavelength must correspond to a spectral absorption line. On the other hand, the communication wavelength is selected partially because of its high atmospheric transmission since communications from space to ground is an important application. Therefore, communication wavelengths are more propitious to the study of refractive-index irregularities.

### 5.3. Sensors

Share is also possible for measurement devices. In a communication terminal, optical-tracking sensors can provide valuable data on the angle of arrival and scintillation. Takayama et al. have reported such data from an occultation of the ARTEMIS-OICETS link [11]. Combined data on wavefront and optical power contain essential information on the dynamic structure of the air. Bandwidth requirements for measuring atmospheric fluctuations may be higher than those for tracking. On a lasercom satellite, tracking sensors have generally a sampling rate on the order of 1 kHz. Significant averaging of atmospheric fluctuations might take place over a 1-ms exposure, especially at low altitudes.

## 6. Conclusion

Whereas optical communications between satellites are perturbed by the atmosphere, optical limb sounding provides important atmospheric data. To reduce costs, atmospheric measurement devices should take advantage of optical space communication technologies whenever synergies are possible.

Although the troposphere can reveal some of its structure through occultations, the stratosphere is easier to study because of its lower attenuation. Optical characteristics of the stratosphere are of interest not only for inter-satellite laser links but also for future laser links involving high-altitude platforms (HAPs). Links between a HAP and a satellite, or between two HAPs, are thought indeed to be promising lasercom applications [13].

## References

1. A. S. Gurvich and V.L. Brekhovskikh, "Study of the turbulence and inner waves in the stratosphere based on the observations of stellar scintillations from space: A model of scintillation spectra", *Waves in Random Media*, 11, 3, 163-181 (2001)
2. A. S. Gurvich and I. P. Chunchuzov, "Parameters of the fine density structure in the stratosphere obtained from spacecraft observations of stellar scintillations," *J. Geophys. Res.* **108**(D5), 4166 ACL 6-1-ACL 6-4 (2003).
3. E. Kyrölä, et al., "GOMOS on Envisat: An overview". *Advances in Space Research*, 33:1020-1028 (2004)
4. V. F. Sofieva, A. S. Gurvich, F. Dalaudier, and V. Kan, "Reconstruction of internal gravity wave and turbulence parameters in the stratosphere using GOMOS scintillation measurements", *J. Geophys. Res.*, 112, D12113 (2007)
5. G. Kirchengast, "Occultations for Probing Atmosphere and Climate: Setting the Scene" in *Occultation for Probing Atmosphere and Climate*, Editors: G. Kirchengast, U. Foelsche, A.K. Steiner, Springer, Berlin-Heidelberg-New York, 1-8 (2004)
6. B. Mayer, S. Shabdanov, D. Giggenbach, "Electronic Database of atmospheric absorption coefficients", DLR-internal report by DLR-IPA and DLR-IKN-DN-OCG, DLR-Oberpfaffenhofen, December 2002, based on the atmospheric constituents profiles according to "G.P. Anderson, et al: AFGL Atmospheric Constituent Profiles (0-120km), AFGL-TR-86-0110, Hanscom Air Force Base, MA 01736, 1986".
7. R. Woo, A. Ishimaru, and F.-Ch. Yang, "Radio scintillations during occultations by turbulent planetary atmospheres," *Radio Sci.* 15, 695-703 (1980)
8. L. Andrews, R. Phillips, *Laser Beam Propagation through Random Media*, 2<sup>nd</sup> Edition, SPIE Press, Bellingham, WA, (2005).
9. J. W. Hardy, *Adaptive Optics for Astronomical Telescopes*, New York: Oxford University Press, 1998.
10. C. Robert, J. -M. Conan, V. Michau, J. -B. Renard, C. Robert, and F. Dalaudier, "Retrieving parameters of the anisotropic refractive index fluctuations spectrum in the stratosphere from balloon-borne observations of stellar scintillation," *J. Opt. Soc. Am. A* **25**, 379-393 (2008)
11. Y. Takayama, T. Jono, Y. Koyama, N. Kura, K. Shiratama, B. Demellenne, Z. Sodnik, A. Bird, and K. Arai, "Observation of atmospheric influence on OICETS inter-orbit laser communication demonstrations", *Proc. SPIE 6709*, 67091B (2007)
12. A. S. Gurvich, V. F. Sofieva, and F. Dalaudier, "Global distribution of CT2 at altitudes 30-50 km from space-borne observations of stellar scintillation", *Geophys. Res. Lett.*, 34, L24813 (2007).
13. N. Perlot, E. Duca, J. Horwath, D. Giggenbach, E. Leitgeb, "System requirements of optical HAP-satellite links", *6th Symposium on Communication Systems, Networks and Digital Signal Processing* (2008)